https://doi.org/10.37434/tpwj2022.06.06

EFFECT OF DEFORMATION OF MOLTEN METAL DROPLETS ON THEIR MOTION AND HEATING IN LIQUID SLAG

I. Krivtsun[1], V. Sydorets[1], G. Stovpchenko[1], G. Polishko[1], A. Sybir[2], L. Medovar[1]

[1]E.O. Paton Electric Welding Institute of the NASU
11 Kazymyr Malevych Str., 03150, Kyiv, Ukraine
[2]National Metallurgical Academy of Ukraine
4 Gagarin Prosp., 49600, Dnipro, Ukraine

ABSTRACT

The mathematical models describing motion and heating of molten metal droplets in a liquid slag layer at the process of traditional electroslag remelting have been developed, assuming that the droplets have a spherical shape or deform to a spheroids flattened in their movement direction. The deformation of metal droplets impacts the velocity of their motion, making more efficient their heating while falling through the molten slag layer because of the bigger midsection and surfase areas of the deformed droplets at the same volume and mass. The differences between the predicted characteristics of motion and heat up of spherical and deforming droplets in the slag layer are more significant for the droplets of large size.

KEYWORDS: electroslag remelting; mathematical modeling; consumable electrode; droplets; motion; deformation; heating

INTRODUCTION

Both the metal and slag droplets usually arise at pyrometallurgical processes, including various refining and welding methods. Droplets quantity and their size define the intensity and completeness of heat and mass transfer in these processes. The knowledge on behaviour of droplets allows optimize the conditions of chemical interactions and heat exchange between phases involved (gas, metal and slag). The behaviour of molten metal droplets at their motion in a liquid slag and vice versa at metal refining is the most often subject of investigation [1–6].

The drag coefficient is the crucial parameter for analysis of the dynamics of liquid metal particles in motion through different media. This coefficient is determined by the Stokes formula (usually for the movement of spherical particles at small Reynolds numbers) or by more complex criterion dependences considering the change in flow nature at particle size and velocity growing [7–9]. In the most cases, a moving droplet is assumed as a solid-state sphere of perfect regular shape. However, the motion of a liquid particle (like a molten metal droplet falling in a slag layer at the electroslag remelting process) has distinctive differences, namely, the change of its shape at motion and, accordingly, the drag force acting on it. The movement of deformable droplets can be modeled using numerical methods [10] allowing to estimate the velocity fields both outside and inside a droplet. However, this approach is quite complicated.

Evaluation of the size of droplets formed in the conditions of the electroslag remelting (ESR) processes on a consumable electrode is considered in many works [11–15]. Usually, the characteristics of a droplet motion in the slag layer is made using the criterion dependences of the drag coefficient for the spherical shape droplet (with no deformation).

In this work the simplified mathematical models allowing numerical evaluation of motion and heating of the molten metal droplets detached from the end of a consumable electrode under the conditions of ESR processes have been developed, taking into account possible changes in the droplet shape while falling in

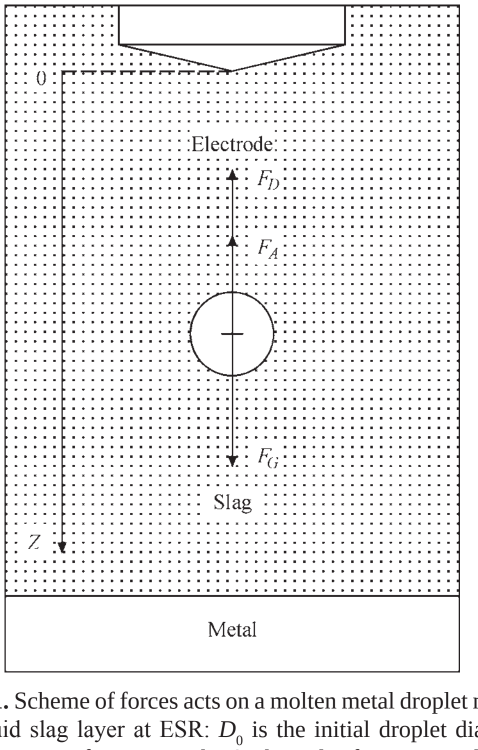

Figure 1. Scheme of forces acts on a molten metal droplet moving in a liquid slag layer at ESR: D_0 is the initial droplet diameter; F_G is the gravity force; F_A is the Archimedes force; F_D is the drag force

a liquid slag layer. Figure 1 shows the scheme of the above mentioned process.

The main parameters of liquid slag and metal droplets used in simulation the following:

- slag (ANF-29): density (ρ_s) — 2780 kg/m^3; specific heat capacity (C_s) — 1200 J/(kg·K); coefficient of dynamic viscosity (η_s) — 0.01965 Pa·s; coefficient of thermal conductivity (χ_s) — 6 W/(m·K); slag temperature (T_s) — 2073 K;
- metal (Steel 45): density (ρ_m) — 7000 kg/m^3; specific heat capacity (C_m) — 600 J/(kg·K); coefficient of dynamic viscosity (η_m) — 0.003 Pa·s; coefficient of thermal conductivity (χ_m) — 35 W/(m·K); coefficient of surface tension (σ_m) — 1.1 N/m; initial temperature of the droplet (T_m) — 1823 K.

MODELLING OF METAL DROPLETS MOTION IN LIQUID SLAG

The droplets detached from the consumable electrode surface move in a liquid slag layer under the gravity force and also are affected by Archimedes and hydrodynamic drag forces (Figure 1). The equation of the movement of a droplet can be written as:

$$\rho_m V\frac{du}{dt}=V(\rho_m-\rho_s)g-C_D S\frac{\rho_s u^2}{2};\ t\ge 0, \tag{1}$$

where V is the droplet volume; $u=dz/dt$ is its velocity; t is the time counted from the moment of the droplet detachment; g is the acceleration of gravity; C_D is the drag coefficient, which depends on the Reynolds number; S is the midsection area of the droplet. At the initial moment ($t = 0$), we will assume that the droplet is spherical and has a diameter D_0 (radius r_0) and zero velocity ($u = 0$).

To estimate the effect of molten metal droplet deformation on its motion in a liquid slag, we consider two cases: the droplet remains spherical form in the process of its movement; the droplet changes its shape (deforms), preserving the same volume as the original spherical droplet.

In the first case, concerning that $V=\frac{4}{3}\pi r_0^3;\ S=\pi r_0^2$, the equation (1) can be rewritten as:

$$\frac{du}{dt}=\frac{\rho_m-\rho_s}{\rho_m}g-C_D\frac{\rho_s}{\rho_m}\frac{3u^2}{4D_0} \tag{2}$$

with the initial condition

$$u|_{t=0}=0. \tag{3}$$

The drag coefficient of a spherical droplet can be expressed by the following criteria dependences [4]:

$$C_{D,sphere}=\begin{cases}\frac{24}{\mathrm{Re}}, & \mathrm{Re}<0,2;\\ \frac{24}{\mathrm{Re}}+3.6\,\mathrm{Re}^{-0.317}, & 0.2<\mathrm{Re}<4;\\ \frac{24}{\mathrm{Re}}+4\,\mathrm{Re}^{-0.333}, & 4<\mathrm{Re}<400;\\ \frac{24}{\mathrm{Re}}+5.48\,\mathrm{Re}^{-0.573}+0.36, & 400<\mathrm{Re}<10^4,\end{cases} \tag{4}$$

Here $\mathrm{Re}\frac{\rho_s u D_0}{\eta_s}$ is the Reynolds number for a droplet moving in a liquid slag.

When performing the numerical calculation, the initial diameter of the droplet D_0 was varied in the range of 2–10 mm. The depth of the slag pool L (distance from the end of the electrode to the metal surface) was constant and equal to 200 mm. All calculations were performed in the following ranges of variables: $0 < t < 1.5$ s; $0 < z < 1000$ mm. The calculated velocity of spherical droplets of small ($D_0 = 2$ mm) and large ($D_0 = 10$ mm) diameter are shown in Figure 2.

These plots show that a spherical droplet of 2 mm reaches its constant (maximum) velocity 0.153 m/s in 0.1 s of its falling (Figure 2, *a*, curve *1*) at a distance from the electrode of about 12 mm (Figure 2, *b*, curve *1*), which is much less than the selected depth of the liquid slag layer. The droplet of 10 mm in diameter moves much faster than the previous one. It reaches its constant speed of 0.641 m/s after 0.3 s (Figure 2, *a*, curve *2*) at a distance from the electrode

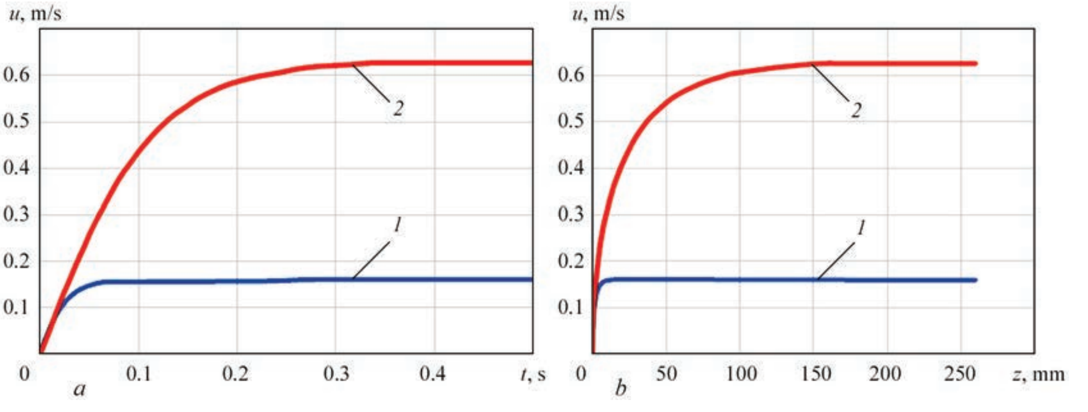

Figure 2. Dependence of velocity of spherical droplets with an initial diameter of 2 mm (*1*) and 10 mm (*2*), on time (*a*) and distance travelled (*b*)

of about 150 mm (Figure 2, *b*, curve *2*), commensurate with the usual depth of a slag pool in commercial ESR processes.

In the case, when a droplet of liquid metal deforms during motion in a slag layer, its shape can be represented as a linear superposition of eigenmodes of natural oscillations of its surface. Under the condition of axially symmetric deformation, it can be presented as:

$$\frac{r_s(\vartheta,t)}{R_0}=1+\sum_{n=2}^{\infty}a_n(t)P_n(\cos\vartheta), \qquad (5)$$

where $r = r_s(\vartheta, t)$ is the equation of a droplet surface in the polar coordinates r, φ, $\vartheta\}$; $P_n(\cos\vartheta)$ is the Legendre polynomials. The equations for determining the dependences of the coefficients of the decomposition (5) on time have the following form [16]:

$$\frac{d^2a_n}{d\bar{t}^2}+8(n-1)(2n+1)\frac{1}{\mathrm{Re}_{def}}\frac{da_n}{d\bar{t}}+$$
$$+8n(n-1)(n+2)\frac{1}{We}a_n=-2nC_n;\ n\geq 2. \qquad (6)$$

Here $\bar{t}=\frac{t}{t^*}$ is the dimensionless time, where $t^*=\sqrt{\frac{\rho_m}{\rho_s}}\frac{D_0}{u}$; $\mathrm{Re}_{def}=\frac{uD_0}{\eta_m}\sqrt{\rho_m\rho_s}$ is the Reynolds number for metal flow inside the droplet; $\mathrm{We}=\frac{\rho_s u^2 D_0}{\sigma_m}$ is the Weber number; C_n are the coefficients of decomposition of the pressure distribution $p_s(\vartheta)$ over the droplet surface

$$\frac{p_s(\vartheta)-p_\infty}{(\rho_s/2)u^2}=\sum_{n=2}^{\infty}C_nP_n(\cos\vartheta). \qquad (7)$$

The experimental dependences of the coefficients C_n in the decomposition (7) on the Reynolds number for the most significant eigenmodes of droplet surface oscillations (n = 2–5) are shown by Schmehl in [16]. As the result the following dependencies for turbulent, non-stationary, asymmetric stationary and laminar flows were obtained: $C_2 = 0.45 + 0.55\exp(-0.15\,\mathrm{Re}^{0.36})$; $C_3 = 0.45 - 0.45\exp(-5.2\cdot10^{-2}\,\mathrm{Re}^{0.63})$; $C_4 = 0.17 - 0.17\exp(-3.9\cdot10^{-5}\,\mathrm{Re}^{1.45})$; $C_5 = -0.07 + 0.07\exp(-5.6\cdot10^{-5}\,\mathrm{Re}^{1.93})$.

The most significant mode (n = 2) of droplet surface oscillations gives enough accurate evaluation of the impact of their deformation on motion speed in liquid slag. So we can assume that the molten metal droplet, having initial spherical shape, deforms and acquires a form of a flattened (in motion direction) spheroid. The spheroid is a rotation body formed by the ellipse (with $a > c$ semi-axes) revolving around the minor axis as shown in Figure 3.

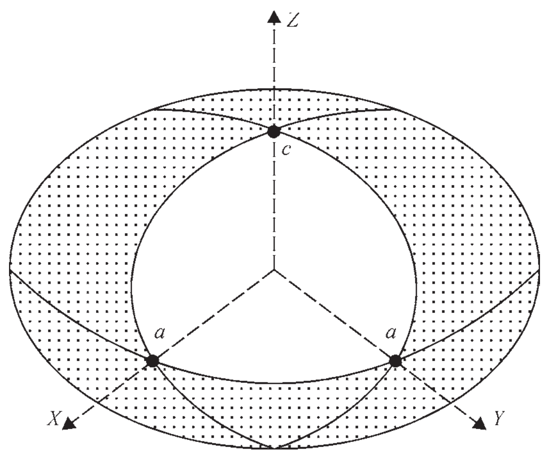

Figure 3. The appearance of a flattened spheroid

The equation of motion (1) sustains the same because the droplet's volume (mass) is constant. The area of the midsection and the drag coefficient of deformed droplets change.

The coefficient characterises a nonsphericality of the deformed droplet shape can be expressed as

$$y=\frac{D}{D_0}=\frac{a}{r_0}\geq 1, \qquad (8)$$

where D is the bigger diameter of the spheroid. Using this coefficient the equation (1) can be rewritten as

$$\frac{du}{dt}=\frac{\rho_m-\rho_s}{\rho_m}g-\bar{C}_D\frac{\rho_s}{\rho_m}\frac{3u^2y^2}{4D_0}, \qquad (9)$$

with the initial condition (3). From the condition of volume preserving for droplets at deformation from the initial spherical shape to a flattened spheroid, it follows that $a = r_0 y$, $c=\frac{r_0}{y^2}$ and the surface area of the deformed droplet is determined as follows:

$$S_s=2\pi a\left(a+\frac{c^2}{\sqrt{a^2-c^2}}\ln\frac{a+\sqrt{a^2-c^2}}{c}\right). \qquad (10)$$

This area will be further compared with the surface area of the original spherical droplet $S_{s_0}=4\pi r_0^2$ using the ratio $S=\frac{S_s}{S_{s_0}}$.

To calculate the drag coefficient of the deformed droplet included in equation (9), we will use the following dependence [16]:

$$\bar{C}_D=(1-f)C_{D,\,sphere}+fC_{D,\,disc}. \qquad (11)$$

Here $f = 1 - E^2$, where $E=\frac{c}{a}=\frac{1}{y^3}$ is the ratio of a small semi-axis of a flattened spheroid to the large one

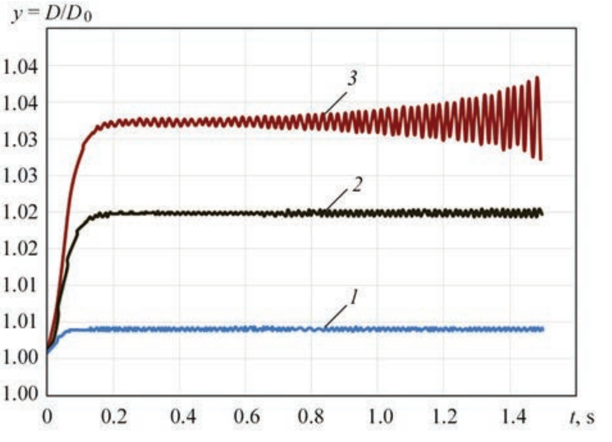

Figure 4. Dependences of the nonsphericality coefficient for the molten metal droplets on time at small values of their initial diameter: *1* — $D_0 = 2$; *2* — 4 ($F = 62.5$ Hz); *3* — 5 mm ($F = 45.0$ Hz)

(in the limiting cases we have: for the sphere $E = 1$, for an infinitely thin disk $E = 0$). The value $C_{D,\ sphere}$ is calculated by the formulas (4) at $\mathrm{Re} = \overline{\mathrm{Re}}$, where $\overline{\mathrm{Re}} = \frac{\rho_s u D_0 y}{\eta_s}$ is the Reynolds number that is calculated taking into account the change in a diameter of the midsection of a droplet, and the drag coefficient of the thin disk, which is calculated by the formula [16]:

$$C_{D,disc} = 1.1 + \frac{64}{\pi \overline{\mathrm{Re}}}. \quad (12)$$

To determine the $y(t)$ value, the first equation (6) (at $n = 2$) can be written in the form [16]:

$$\frac{d^2 y}{d\bar{t}^2} + \frac{40}{\mathrm{Re}_{def}} \frac{dy}{d\bar{t}} + \frac{64}{\mathrm{We}}(y-1) = \\ = 0.9 + 1.1\exp\left[-0.15\overline{\mathrm{Re}}^{0.36}\right] \quad (13)$$

with the initial conditions

$$y|_{\bar{t}=0} = 1; \qquad \left.\frac{dy}{d\bar{t}}\right|_{\bar{t}=0} = 0. \quad (14)$$

The results of modelling behaviour of the molten metal droplets having different initial diameters with considering their deformation at movement in the slag layer are presented in Figures 4–7.

As follows from the calculated data shown in Figure 4, droplets of a size up to 4 mm almost preserves the initial spherical shape during their motion in the liquid slag layer. They experience weak oscillations of the shape with a frequency F that reduces with D_0 increase (4 mm $F = 62.5$ Hz; 5 mm $F = 45$ Hz). A droplet with an initial diameter of 5 mm undergoes deformation in the oscillating mode with a growing amplitude. The average value of the degree of deformation $\delta = \frac{D - D_0}{D_0}$ of such a droplet amounts about 3 % (Figure 4, curve *3*).

As shown in Figure 6, for larger droplets ($D_0 = 6–10$ mm) the degree of deformation grows with an increase in D_0 at a corresponding rise in the amplitude of oscillations of the droplet surface, and these oscillations themselves become aperiodic starting from a certain moment of time (or after passing the appropriate distance in a liquid slag), what can lead to the disintegration of the droplet into smaller fragments. For example, the Weber number for the droplets with the initial diameter of 10 mm, reaches values close to critical (We > 5) already at $t = 0.2$ s. Dependences of the nonsphericality coefficient for the molten metal droplets on time at small values of their initial diameter are shown in Figure 5, *a*.

The calculation data shown in Figure *6*, a, illustrate the degree of maximum deformation of molten metal droplets of various initial diameters during their motion in a liquid slag for the time moment of 1.2 s.

The significant deformation of a large droplet ($D_0 = 8–10$ mm) increases their surface area in compare of the initial spherical droplet, as shown in Figure 6, *b*. This can significantly intensify their heat exchange and chemical interaction with a liquid slag.

The effect of deformation of metal droplets of different initial diameters on the velocity of their motion in a liquid slag is illustrated in Figure 7.

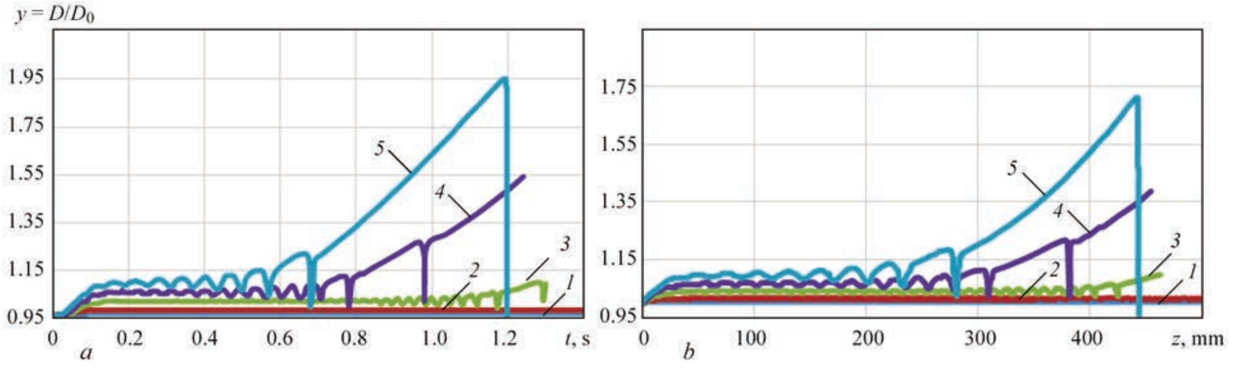

Figure 5. Dependences of the nonsphericality coefficient of molten metal droplets on time (*a*) and distance travelled (*b*) at different initial diameters: *1* — $D_0 = 2$; *2* — 4; *3* — 6; *4* — 8; *5* — 10 mm

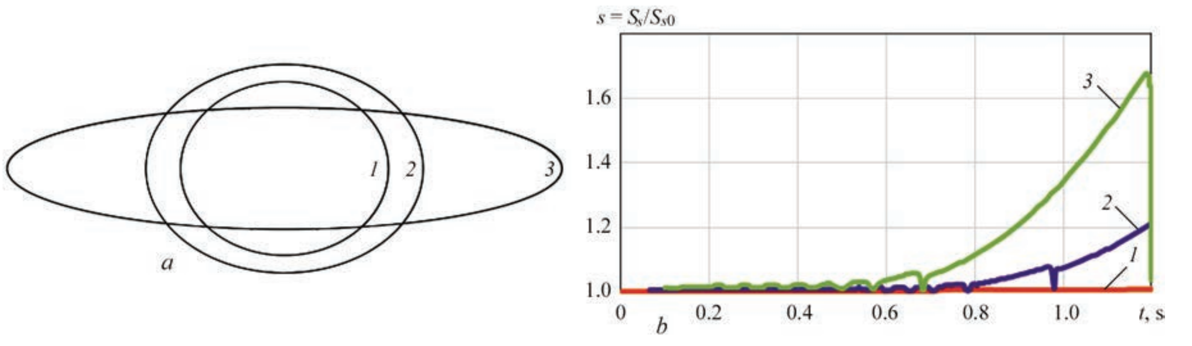

Figure 6. The shape of droplets at 1.2 s from the beginning of their motion and dependence of surface area of deformed metal droplets on time at various values of initial droplet diameter: *1* — D_0 = 6; *2* — 8; *3* — 10 mm

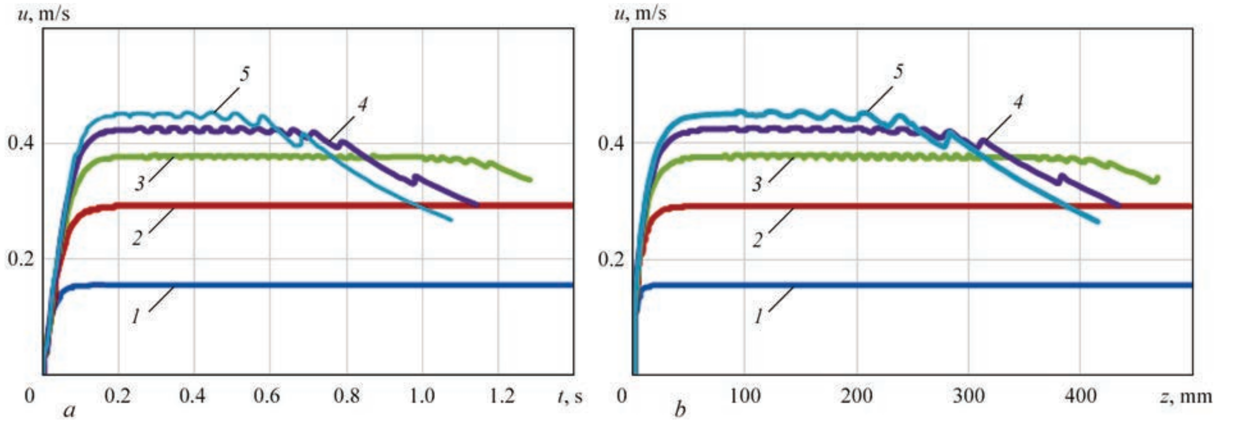

Figure 7. Dependences of velocity of deformed metal droplets on time (*a*) and passed distance (*b*) at various values of initial droplet diameter: *1* — D_0 = 2; *2* — 4; *3* — 6; *4* — 8; *5* — 10 mm

The calculated dependences prove that the small droplets (diameter of 2–4 mm) do not deform sufficiently while their motion (Figures 4, 5). For example, droplets with initial diameter 2 mm reach a constant speed of 0.153 m/s in 0.1 s (at a distance about 12 mm from the electrode), which is similar with the correspondent spherical shape droplets (Figure 2, *a*, *b*, curves *1*). As for the droplets of a larger initial diameter (D_0 = 6–10 mm), they move more slowly than the corresponding spherical droplets because they are subjected to significant deformation at their motion (Figures 5, 6). For example, deformed droplets of 10 mm in diameter reach a speed of 0.450 m/s at a distance of about 100 mm from the surface of the slag pool for 0.2 s, which is significantly lower than the corresponding values for the same size spherical droplets (Figure 2, *a*, *b*, curves *2*). Taking into account that the large droplets deformation occurs in an oscillating mode with an increasing amplitude (Figure 5), their speed decreases (Figure 7) due to changes in the drag force acting on them.

Analysing the results of simulation of molten metal droplets movement in the slag layer at ESR, it should be noted that at the selected depth of the slag pool (L = 200 mm), the noted features of the motion of droplets associated with their deformation became sufficient for large droplets with an initial diameter of more than 8 mm (Figures 5, *b*, 7, *b*).

MODELLING OF METAL DROPLETS HEATING

Assuming that the temperature of the metal in the volume of a droplet has an uniform distribution, the equation that describes heating of a metal droplet during its motion in a liquid slag can be written as:

$$\rho_m V C_m \frac{dT_m}{dt} = S_s \alpha (T_s - T_m);\ t \geq 0, \tag{15}$$

where T_m is the metal temperature; α is the coefficient of convective-conductive heat exchange, and other designations correspond to those accepted earlier.

If a droplet in the process of its motion preserves a spherical shape, then the equation (15) can be written as:

$$\frac{dT_m}{dt} = \frac{6\alpha}{\rho_m C_m D_0}(T_s - T_m) \tag{16}$$

with the initial condition

$$T_m\big|_{t=0} = T_0, \tag{17}$$

To determine the heat exchanger coefficient α, the Nusselt criterion $\mathrm{Nu} = \frac{\alpha D_0}{\chi_s}$ was used. In the case of

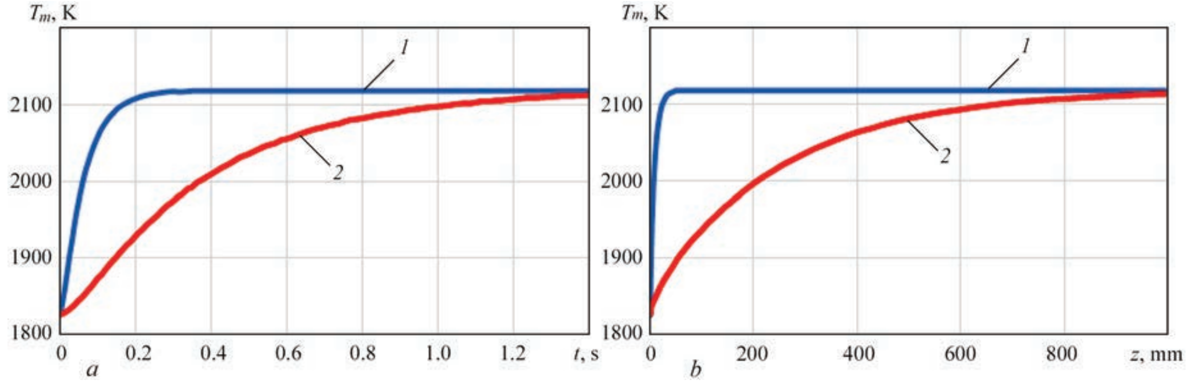

Figure 8. Dependence of temperature of spherical droplets with an initial diameter of 2 mm (*1*) and 10 mm (*2*), on time (*a*) and distance travelled (*b*)

a spherical shape of the droplet, the criterion dependence have the form [4]:

$$\mathrm{Nu} = 2.0 + 0.6\mathrm{Re}^{0.5}\mathrm{Pr}^{0.333}. \quad (18)$$

Here $\mathrm{Pr} = \frac{C_s \eta_s}{\chi_s}$ is the Prandtl number. The Reynolds number was determined considering the change in the droplet velocity depending on the time according to the accepted model of its motion.

The results of simulation of heating of undeformed (spherical) metal droplets of various initial diameters falling in a liquid slag, shown in Figure 8, demonstrate that small droplets are heating up from the initial temperature (1823 K) to the slag temperature (2073 K) much faster than large droplets. For example, a droplet with a diameter of 2 mm reaches the temperature of the slag after 0.25 s (Figure 8, *a*, curve *1*) at a distance of about 40 mm (Figure 8, *b*, curve *1*) from the electrode tip, which is significantly lower than the selected depth of the slag pool.

A droplet with a diameter of 10 mm is heating up much more slowly, and therefore, while passing the entire depth of the slag pool (L = 200 mm), its temperature does not exceed 1980 K (Figure 8, *a*, *b*, curves *2*).

Let us consider now the peculiarities of heating metal droplets during their motion in a liquid slag taking into account their deformation. As previously, we will approximately assume that a droplet in the movement process acquires the shape of a flattened spheroid. Homogeneous heating of a liquid metal droplet deformed in such a way is described by a differential equation

$$\frac{dT_m}{dt} = \frac{3\bar{\alpha} y^2}{\rho_m C_m D_0} \times \left[1 + \frac{1}{y^3\sqrt{y^6 - 1}} \ln\left(y^3 + \sqrt{y^6 - 1}\right)\right](T_s - T_m) \quad (19)$$

with the initial condition (17). Here $y = \frac{D}{D_0}$ is the coefficient of a nonsphericality of droplet; $\bar{\alpha}$ is the heat exchange coefficient for a spheroid, in the determination of which the criterion dependence (18) was used, taking into account that the Nusselt number $\overline{\mathrm{Nu}} = \frac{\bar{\alpha} D_0 y}{\chi_s}$ and the Reynolds number $\overline{\mathrm{Re}} = \frac{\rho_s u D_0 y}{\eta_s}$ were calculated for the midsection diameter of a deformed droplet.

The calculated temperatures for the deformed droplets having various initial diameters on the time and distance travelled in the slag are shown in Figure 11.

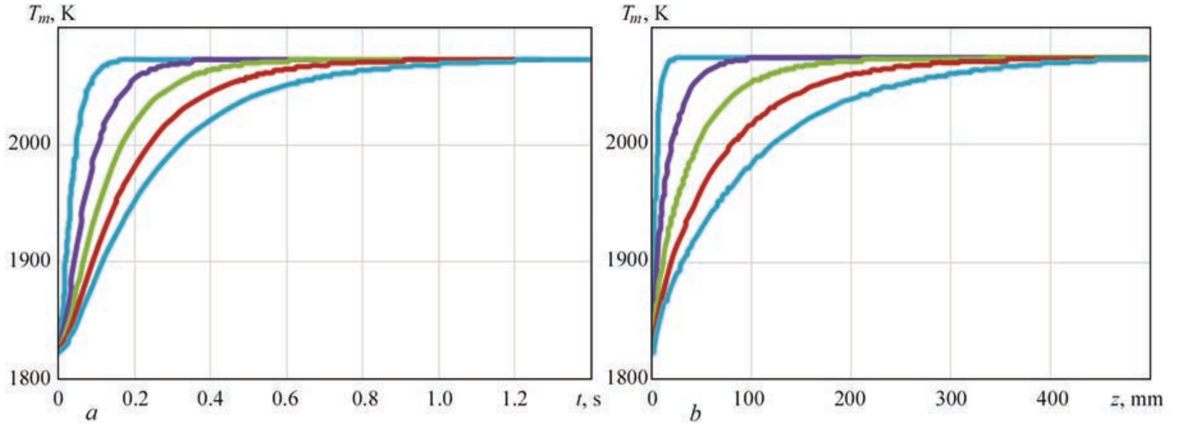

Figure 9. Dependences of temperature of deformed metal droplets on time (*a*) and distance traveled (*b*) at various values of initial droplet diameter: *1* — D_0 = 2; *2* — 4; *3* — 6; *4* — 8; *5* — 10 mm

Table 1. Results of numerical simulation of the processes of motion and heating of molten metal droplets in a liquid slag

D_0, mm	Motion								Heating					
	u_{max}, m/sec		z, mm at $u = u_{max}$		t, s at $u = u_{max}$		t, s at z = 200 mm		z, mm at $T_m = T_s$		t, s at $T_m = T_s$		T_m, K at z = 200 mm	
	SD*	DD**	SD	DD	SD	DD	SD	DD	SD	DD	SD	DD	SD	DD
2	0.153	0.153	12	12	0.10	0.10	1.33	1.33	40	40	0.30	0.20	2073	2073
4	–	0.289	–	30	–	0.15	–	0.74	–	90	–	0.38	–	2073
6	–	0.375	–	60	–	0.16	–	0.58	–	220	–	0.60	–	2070
8	–	0.420	–	80	–	0.18	–	0.53	–	370	–	0.93	–	2050
10	0.641	0.450	150	100	0.30	0.20	0.40	0.51	1000	450	1.60	1.20	1980	2010

*SD — spherical droplet. **DD — deformable droplet.

As follows from the data in Figures 8, *a*, *b*, and 9, an unsignificant deformation of small droplets at motion in the liquid slag (Figure 4) does not significantly change their heating compared to those for spherical droplets. For the convenience of readers, Table 1 shows generalised data on the obtained calculation results.

Deformation of large droplets makes an increasingly significant effect on their heating in liquid slag. For example, a deformed droplet of 10 mm in diameter heats to a slag temperature for a time of about 1.3 s (a distance about 500 mm from the electrode tip). Whereas for a spherical droplet (the deformation is not taken into account), the mentioned conditions ($T_m = T_s$) are met at $t \geq 1.6$ s, $z \geq 1000$ mm (Figure 8, a, b, curves 2). This allows concluding the intensification of heat exchange between liquid slag and metal droplets due to their shape changing.

The results of a numerical study of the moving and heating processes of metal droplets of various initial diameter in a liquid slag with and without taking into account their deformation is valuable for better understanding the heat and mass transfer pricesses in ESR.

CONCLUSIONS

1. Mathematical modeling and numerical simulation of the processes of moving and heating of molten metal droplets in a liquid slag at ESR were completed. Two cases of droplet's behaviour have been considered: when it preserves the initial spherical shape while falling in the slag; when it deforms taking the form of a flattened (in the direction of motion) spheroid. The deformation of droplets affects velocity (duration) of their motion in the slag layer because it increases the drag force acting on a droplet, as well as intensifies their heating and metallurgical interaction with a molten slag because it increases the surface area of a droplet (while maintaining its volume).

2. The deformation of droplets of small diameter (up to 5 mm) occurs by harmonic oscillations of their surface at the frequency range of 50–100 Hz. This frequency increases at a droplet diameter decreasing. The tiny droplets deformation is low (up to 3 %) and almost does not affect on their motion and heating in a liquid slag compared to the corresponding spherical shape droplets.

3. Droplets of large diameter (6–10 mm) undergo a significant deformation, which degree is the bigger, the greater a droplet diameter. The oscillations of its surface become aperiodic with growing amplitude (for a droplet with a diameter of 10 mm, the degree of deformation can reach 75%), which can eventually lead to decomposition of such droplets into smaller ones. Deformed droplets with an initial diameter of 10 mm reach a maximum velocity of 0.45 m/s (for 0.2 s at a distance of 100 mm from the electrode), much lower than the limiting speed of a corresponding spherical droplet (0.64 m/s), and then their velocity decreases.

4. Due to the surface area growing and velocity reduction for droplets of a larger diameter, their heating in the slag layer becames more efficient than for the corresponding spherical droplets. For example, the spherical droplet of 10 mm in diameter reaches the slag temperature of about 1.6 s at a distance of more than 1000 mm from the electrode. In contrast, for deformed droplets, this occurs in 1.2 s at the distance of 450 mm. At the given slag pool depth equals 200 mm, a deformable droplet of 10 mm in diameter is heated only to a temperature of 2010 K, which is more than 60 K lower than the slag temperature.

REFERENCES

1. Medovar, B.I., Tsykulenko, A.K., Shevtsov, V.L. (1986) *Metallurgy of electroslag process*. Kyiv, Naukova Dumka [in Russian].
2. Gulyaev, I.P., Dolmatov, A.V., Kharlamov, M.Yu. et al. (2015) Arc-plasma wire spraying: An optical study of process phenomenology. *J. of Thermal Spray Technology*, 24(**4**), 659–670.
3. Chaulet, J., Kharicha, A., Charmond, S. et al. (2020) A 2D multiphase model of drop behavior during electroslag remelting. *Metals*, **10**, 490. DOI: https://doi.org/10.3390/met10040490
4. Clift, R., Grace, J.R., Weber, M.E. (1978) *Bubbles, drops and particles*. New-York, London, Academic Press.
5. Michaelides, E.E. (2006) *Particles, bubbles & drops*: Their motion, heat and mass transfer. World Scientific Publ.

6. Medovar, L.B., Stovpchenko, G.P., Sybir, A.V. (2020) Comparison of conditions of mass exchange in electroslag processes with consumable electrode and liquid metal. *Uspekhi Fiziki Metallov*, **4**, 481–500 [in Russian]. DOI: https://doi.org/10.15407/ufm.21.01.001
7. Happel, J., Brenner G., (1976) *Hydrodynamics under small Reynolds numbers*. Moscow, Mir [in Russian].
8. Brooks, G., Subagyo, Y. Pan (2005) Modeling of trajectory and residence time of metal droplets in slag–metal–gas emulsions in oxygen steel making. *Metall. and Material Transact. B*, **36**, 525–535. DOI: https://doi.org/10.1007/s11663-005-0044-x
9. *Nanda* Kishore, Sai Gu (2011) Momentum and heat transfer phenomena of spheroid particles at moderate Reynolds and Prandtl numbers. *Heat Mass Transfer*, 54(**11–12**), 2595–2601. DOI: https://doi.org/10.1016/j.ijheatmasstransfer.2011.02.001
10. Yang, C., Mao, Z. (2014) *Numerical simulation of multiphase reactors with continuous liquid phase*. Academic Press.
11. Kharicha, A., Karimi-Sibaki, E., Wu, M. et al. (2018) Review on modeling and simulation of electroslag remelting. *Steel Research Int*., 89(**1**).
12. Dudko, D.A., Rublevsky, I.N. (1961) About drop transfer of electrode metal in electroslag welding. *Avtomatich. Svarka*, **4**, 24–31 [in Russian].
13. Polishko, G., Stovpchenko, G., Medovar, L., Kamkina, L. (2019) Physicochemical comparison of electroslag remelting with consumable electrode and electroslag refining with liquid metal. *Iron Making & Steel Making*, 46(**8**), 789–793. DOI: https://doi.org/10.1080/03019233.2018.1428419
14. Klyuev, M.M., Volkov, S.V. (1984) *Electroslag remelting*. Moscow, Metallurgiya [in Russian].
15. Klyuev, M.M., Nikulin, A.A. (1970) Speed of movement and degree of heating of the metal drop in slag during electroslag remelting. *Bulleten TsNIICherMet*., **4**, 32–34 [in Russian].
16. Schmehl, R. (2002) Advanced modeling of droplet deformation and breakup for CFD analysis of mixture preparation. In: *Proc. of ILASS-Europe 2002 (Zaragoza, 9–11 September, 2002)*.

ORCID

I. Krivtsun: 0000-0001-9818-3383,
V. Sydorets: 0000-0002-8498-4726,
G. Stovpchenko: 0000-0002-6555-5715,
G. Polishko: 0000-0001-7543-280X,
A. Sybir: 0000-0002-9974-0636,
L. Medovar: 0000-0003-2077-5965

CONFLICT OF INTEREST

The Authors declare no conflict of interest

CORRESPONDING AUTHOR

I. Krivtsun
E.O. Paton Electric Welding Institute of the NASU
11 Kazymyr Malevych Str., 03150, Kyiv, Ukraine.
E-mail: krivtsun@paton.kiev.ua

SUGGESTED CITATION

I. Krivtsun, V. Sydorets, G. Stovpchenko, G. Polishko, A. Sybir, L. Medovar (2022) Effect of deformation of molten metal droplets on their motion and heating in liquid slag. *The Paton Welding J*., **6**, 41–48.

JOURNAL HOME PAGE

https://pwj.com.ua/en

Received: 07.07.2022
Accepted: 15.08.2022